International Journal of Engineering Research and General Science Volume 2, Issue 5, August-September, 2014
ISSN 2091-2730

Catalytic Decomposition of Hydrocarbon Gas over Various Nanostructured Metal oxides for Hydrocarbon Removal and Production of Carbon Nanotubes

M.H.Khedr[a,d], M.I.Nasr[b], K.S.Abdel Halim[b], A.A.Farghali[a,d], N.K.Soliman[c*]

a Chemistry Department, Faculty of Science, Beni-Sueif University, Beni-Suef, Egypt

b Central Metallurgical Research & Development Institute (CMRDI), Minerals Technology, 87 Helwan, Cairo, Egypt

C Basic Science Department, Faculty of Oral and Dental Medicine, Nahda university (NUB), Beni-suef , Egypt

d Material Science and nanotechnology department , faculty of post graduate studies for advanced science, Beni-Sueif University, Beni-Suef, Egypt

* Corresponding author: Assistant lecturer. N.K.Soliman, (E-mail: nofal_kh7@yahoo.com)

Abstract: Nanosized CuO-CeO_2, CuO-Fe_2O_3, CuO-CeO_2-Al_2O_3 and CuO-Fe_2O_3-CeO_2-Al_2O_3 were prepared by co-precipitation and wet impregnation techniques and were used for Catalytic decomposition of acetylene to produce carbon nanotubes (CNTs). Weight gain technique was used to follow up the catalytic reactions. The results revealed that catalyst chemical composition, catalytic temperature, acetylene flow rate and catalyst's weight have a significant effect on the acetylene conversion percent. It was found that maximum acetylene conversion percent occurs over CuO-CeO_2-Fe_2O_3-Al_2O_3 and CuO-Fe_2O_3 and it increase by increasing, temperature from 400-600^oC, decreasing acetylene flow rate from 150-50 ml/min and increasing catalyst weight from 0.25-1g. With further increase in catalyst weight, acetylene conversion% decrease. The scanning electron microscope (SEM) image shows that some of catalyst particles are observed at the tips of CNTs indicating that its formation proceeds by tip growth mechanism.

` The prepared samples and CNTs were characterized by X-ray diffraction, inductive coupled plasma – atomic emission spectroscopy (ICP-AES), surface area apparatus, Transmission electron microscope (TEM) and SEM.

Keywords - *metal oxides, nanocrystallite, microstructure, hydrocarbon gas, Acetylene, chemical vapor deposition, Carbon nanotubes,*

1. Introduction

Unburned hydrocarbons (HC) are one of the main pollutants released from internal combustion engines and cause many environmental and health problems[1, 2], for example, Volatile organic compounds (VOCs) enter in the formation of ground level ozone ,ozone depletion ,and they act as greenhouse gases[3, 4] . Decomposition of hydrocarbon gases to its constituents is considered to be one of the most important ways to remove such gases. Transition metal oxides showed very high catalytic activity toward the decomposition of hydrocarbon gases to carbon nanotubes [5-7] which have novel properties that have led to realistic possibilities of using them in many applications [8-16].

CNTs have been synthesized by a lot of techniques, such as plasma-enhanced ,arc discharge, laser ablation, and chemical vapor deposition (CVD) of hydrocarbon gases (methane, ethane, and acetylene) at relatively high temperature over a nanocatalysts [17-19] , chemical vapor deposition (CVD) has been extensively used for the production of large scale carbon nanotubes with extraordinary properties with high yield and it can produce CNTs at much lower temperature and with low cost [20-22].

The Effect of temperature on the kinetics of acetylene decomposition over freshly reduced iron oxide nanoparticles for the production of carbon nanotubes was studied by khedr et al [6], The results showed that both the crystal size of iron oxide and catalytic decomposition temperature are very effective on percentage yield of carbon deposited. The percentage yield of the produced CNTs increased by decreasing crystal size of the catalyst from 150 to 35 nm, and increasing acetylene decomposition temperature to certain temperature limit and after that it decrease.

The present work is designated to synthesize various nanostructured metal oxides catalysts for the decomposition of acetylene to produce carbon nanotubes. The influence of different factors such as catalyst chemical composition, catalytic

temperature, acetylene flow rate and weight of catalysts on the rate of catalytic reaction was investigated using weight gain technique. The experimental data were used to clarify the mechanism of the reaction.

2. Experimental

2.1. Catalyst preparation Experiment

Different Nanocrystallite materials of $CuO\text{-}CeO_2$ with molar ratio 5:95 and $CuO\text{-}Fe_2O_3$ with molar ratio1:1, were successfully prepared by co-precipitation route. The metal precursors solutions (Cerium (III) sulphate, cupper (II) sulphate and iron (II) nitrate) with required molar ratios were co-precipitated using potassium hydroxide as a precipitating agent, the precipitating agent was added drop wise to the precursors solutions during ultra sonication for 0.5 hr then the precipitate was washed with distilled water and ethanol, dried at 105^{o}C and finally fired at 500^{o}C for about 3 hrs.

Nano-sized $CuO\text{-}CeO_2$ supported Al_2O_3 is prepared by weight impregnation technique [6] where a catalyst of the composition 40% $CuO\text{-}CeO_2$:60% Al_2O_3 was prepared as follows: a suspension of nanosized $CuO\text{-}CeO_2$ was mixed with Al_2O_3 powder and stirred for 1 hr at 60 ^{o}C to form a paste and to achieve a homogeneous impregnation of catalyst in the support. The impregnate was then dried in an oven at 100 ^{o}C for 1 hr, calcinated at 400 ^{o}C for 3 hrs in a box muffle furnace.

Nano-sized $CuO\text{-}Fe_2O_3\text{-}CeO_2\text{-}Al_2O_3$ with molar ratio 0.26: 0.19: 0.25: 0.3 was prepared by physical mixing of a solid mixture of one mole of $CuO\text{-}Fe_2O_3$ with one mole $CuO\text{-}CeO_2\text{-}Al_2O_3$.

The prepared catalysts were characterized using X-ray phase analysis technique ,The BET surface area apparatus (Quanta chrome NOVA Automated Gas Sorption System), inductive coupled plasma – atomic emission spectroscopy (ICP-AES), Scanning electron microscope and Transmission electron microscope .

Phase identification and crystallite size of the products were determined using X-ray diffraction instrument where the crystallite size (D) has been calculated using Scherer's equation [23]:

$$D = \frac{0.9\lambda}{B\cos\theta}$$

Where B is the full width at half maximum, λ is the X-ray wavelength, and θ is the angle of diffraction

2.2. Hydrocarbon decomposition Experiment

For each acetylene decomposition Experiment, approximately 0.5 g of a catalyst was introduced in to cylindrical alumina cell closed with one end and placed in the central region of a longitudinal furnace.

To determine the most effective catalyst, which gives the highest acetylene conversion% (the highest carbon yield); the catalysts were heated at 600 ^{o}C and carbon nanotubes (CNTs) were synthesized at this temperature by flowing 100ml C_2H_2:700 ml N_2 at these temperature. Decomposition of acetylene over different catalysts was followed using weight gain technique. The efficiency of the prepared catalysts was determined and correlated with operation parameters which comprise; Temperature of reaction, catalyst chemical composition, acetylene flow rate, and catalyst weight. The effect of growth temperature on the acetylene conversion% was also examined for the most effective catalysts in acetylene decomposition at temperature ranging from 400 to 600 ^{o}C. The synthesized CNTs were cooled in N_2 flow and the weight of deposited CNTs was detected using weight gain technique. The catalytic activity of catalyst was measured by measuring acetylene conversion% as follow,

$$\text{Acetylene conversion } \% = \frac{W_t}{W_c} x100$$

Where W_t is the weight of carbon deposited at time t and W_c is the total weight of carbon on hydrocarbon supply passed over the metal oxides catalysts in 30 minutes.The effect of acetylene flow rate and catalyst's weights were investigated using different acetylene inlet concentrations ranging from 50 to 150 ml/min and different catalyst's weights ranging from 0.25 to 2 g over the most effective catalyst in by carrying out the acetylene decomposition reactions at 600 ^{o}C

The synthesized CNTs were identified and characterized using X-ray phase analysis technique, Scanning electron microscope and Transmission electron microscope.

3. Results and discussions

3.1. Characterization of catalysts

The results of phase identification and crystallite size measurements of the prepared catalysts are summarized in Table 1 and Fig. 1. The XRD patterns of $CuO\text{-}Fe_2O_3$ catalysts show that there is no interaction between CuO and Fe_2O_3 and no copper ferrite peaks

were detected. Fig.1(b, c) shows XRD patterns of CuO–CeO_2 catalysts washed with ethanol, CeO_2 of fluorite type oxide structure was observed in all catalysts [24] and no shift in the diffraction lines of CeO_2 could be observed in these catalysts, indicating that there are no solid solutions appeared in the CuO – CeO_2 catalyst [25]. Also XRD results indicate that using Al_2O_3 as support help in decreasing the crystal size of the prepared catalysts and that the addition of KOH as precipitating agent and ethanol as dehydrating agent inhibits the grain growth of CuO–CeO_2 particles, yields nano-structured catalysts (crystal size =12.7 nm) and increases the surface areas of *catalysts* (58.3 m^2 g^{-1} for CuO–CeO_2) as summarized in Table .1. We found also no observable XRD peaks corresponding to CuO in CuO–CeO_2 catalysts. This could indicate that the doped CuO was well dispersed in the CeO_2 surface or it may be amorphous or undetectable amount (about 5%) by XRD

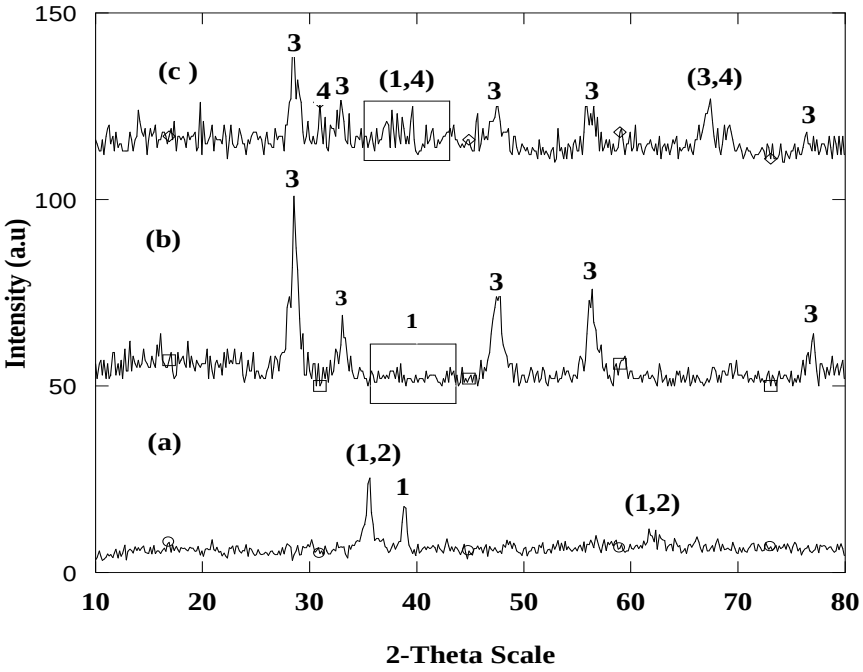

Fig .1. XRD pattern for

(a) CuO-Fe_2O_3 (b) CuO-CeO_2 (c) CuO-CeO_2-Al_2O_3

Where 1, 2, 3 and 4 represent CuO, Fe_2O_3, CeO_2 and Al_2O_3 respectively

Table 1. Crystal sizes and surface area of the prepared catalysts

Catalyst	Sample phases	Crystal size (nm)	Surface area (m^2/g)
CuO-Fe_2O_3	CuO	28.7 nm	15.7
	Fe_2O_3	13.6 nm	
CuO-CeO_2-Al_2O_3	CuO	Nd	58.3
	CeO_2	11.7 nm	
	Al_2O_3	7 nm	
CuO-CeO_2	CuO	nd	Nd
	CeO_2	12.7 nm	

nd means not determined

The results obtained by ICP indicate that the catalysts are well prepared with the proper metal to metal ratios. The results are summarized in table.2.

Table .2. ICP –AES results of the prepared catalysts

Catalyst	Chemical composition	ICP results ratios
1	50% CuO + 50% Fe_2O_3	51% CuO + 49% Fe_2O_3
2	5% CuO + 95% CeO_2	5.1% CuO + 94.9% CeO_2
3	2% CuO + 38% CeO_2+ 60% Al_2O_3	2% CuO + 39.1% CeO_2+ 58.9% Al_2O_3

Fig.2. and Fig.3. shows TEM and SEM images of $CuO\text{-}CeO_2$ supported Al_2O_3 catalyst and $CuO\text{-}Fe_2O_3$ catalyst, from which we can see that the particles are well dispersed and have a regular spherical morphology, the powder was mostly formed in homogenous grains and the $CuO\text{-}Fe_2O_3$ sample seems to be more condensed than $CuO\text{-}CeO_2\text{-}Al_2O_3$, this is confirmed by the pore size distribution shown in Fig.4. The data obtained from the BET surface area apparatus show that the total pore volume is 2.9×10^{-2} CC / g , micro pore volume 6.6×10^{-2} CC / g and average pore diameter 0.02 µm in case of $CuO\text{-}CeO_2\text{-}Al_2O_3$ while in case of $CuO\text{-}Fe_2O_3$ the total pore volume is 7.5×10^{-3} CC / g , micro pore volume 1.3×10^{-2} CC / g and average pore diameter 0.019 µm.

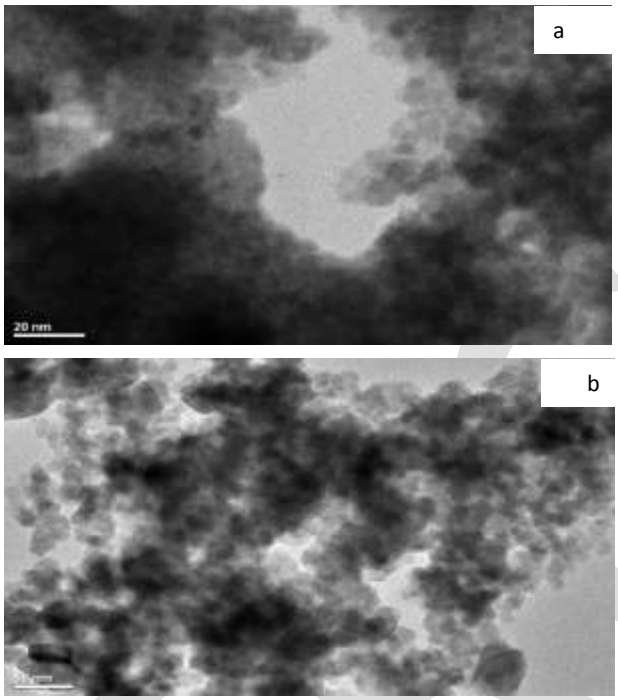

Fig .2. TEM image of
(a) $CuO –CeO_2\text{-} Al_2O_3$ (b) $CuO –Fe_2O_3$

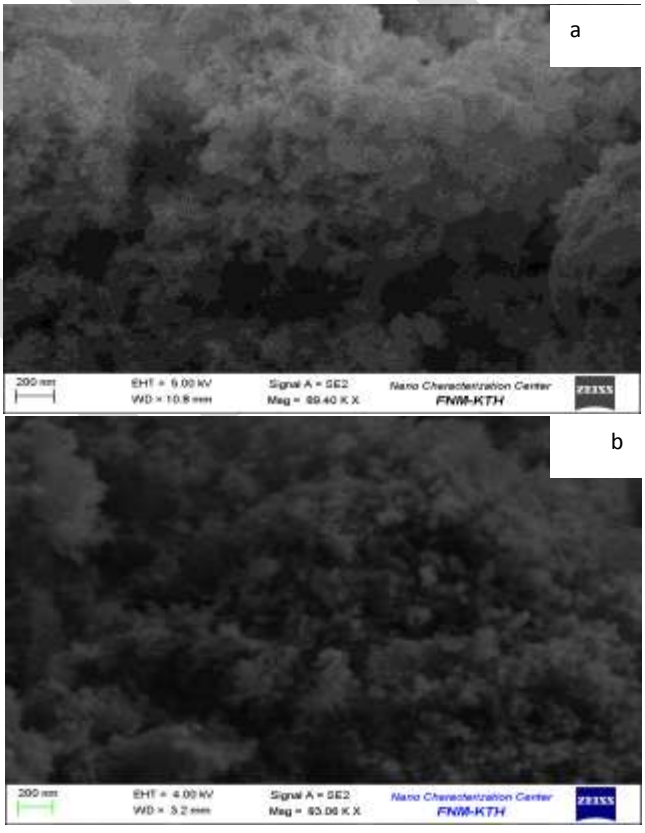

Fig .3. SEM image of

(a) CuO –CeO_2- Al_2O_3 (b) CuO –Fe_2O_3

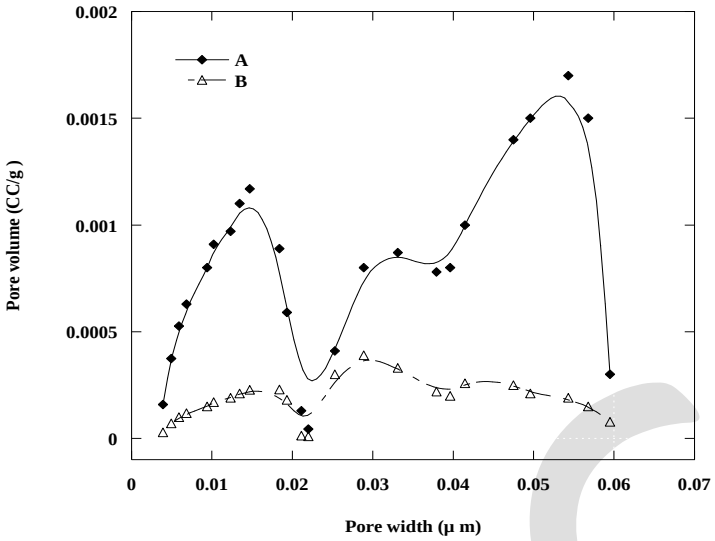

Fig.4. Relation between pore width and pore volume for

(A) CuO -CeO_2-Al_2O_3 (B) CuO Fe_2O_3

3.2. Hydrocarbon decomposition

Hydrocarbon isothermal-decomposition experiments indicate that acetylene gas (with a flow rate 50 ml/min.) decomposes catalytically to carbon and hydrogen at 600 ^oC according to the following equation [6];

$$C_2H_2 = H_2 + 2\,C$$

The acetylene molecules adsorbed on the surface of the catalyst then, a weak bond is formed between the catalyst and the carbon atoms of acetylene molecules then the bonds between carbon atoms on the acetylene molecules are elongated and finally the C-C triple and the C-H bonds is broken and carbon atoms attached together and hydrogen atoms also combined forming the carbon nanotubes and hydrogen gas molecule respectively[6].

3.2.1. Effect of catalyst composition

Catalytic decomposition tests were carried out in the simulated reactor to study the effect of catalyst composition on the removal of acetylene by catalytic decomposition reaction. The decomposition tests were investigated isothermally through the decomposition of acetylene to produce carbon nanotubes as a function of the prepared samples at 600 ^oC and acetylene flow rate 50 ml/min using weight gain technique.

Table 3 shows the effect of catalyst composition on the catalytic decomposition of acetylene. It is found that CuO-CeO_2 and CuO-CeO_2-Al_2O_3 catalysts have no catalytic activity toward acetylene decomposition because there is no type of interaction between metal oxides and ceria as observed from XRD results so they have no catalytic activity [17], while good conversion percent is observed with CuO-CeO_2-Fe_2O_3-Al_2O_3 and this may be attributed to that the metal oxide catalysts supported on alumina, posses certain acidic sites, and the catalytic decomposition of hydrocarbons is proceeded on this sites and hence the catalytic activity of the prepared catalysts toward decomposition of acetylene increase [26] The small crystallite size of the catalysts also enhances the synthesis of dense, long and narrow-diameter CNTs [27] due to increasing the number of active sites at the catalyst surface which in turn enhanced the acetylene decomposition reaction into carbon nanotubes and hydrogen. Accordingly, acetylene conversion % increase [6].

Table .3. the effect of catalyst composition on the catalytic decomposition of acetylene

Catalyst	HC conversion %
CuO-CeO2	No catalytic activity
CuO-CeO_2-Al_2O_3	No catalytic activity
CuO-Fe_2O_3	53.4 %
CuO-Fe_2O_3 -CeO_2-Al_2O_3	68 %

SEM analysis of the produced CNTs over both CuO -Fe_2O_3 and CuO-Fe_2O_3 -CeO_2-Al_2O_3 at 600 ^oC are shown in Fig.5. High dense of CNTs are observed in all the samples .The SEM observations suggest also that the carbon nanotube length is ranging from one to several µm. Several long CNTs were observed in the images and scattered in all the samples and it can be observed that there is a tendency towards the formation of CNT structures of larger diameter at higher temperature. This is in line with other studies and may be attributed to the agglomeration of metal oxides crystallites at higher reaction temperatures to form larger and non-uniform metallic clusters which are responsible for growth of thicker CNTs [28] and some catalytic nanoparticales are also observed at the tips of the carbon nanotubes indicating that CNTs formation occurs by tip growth mechanism

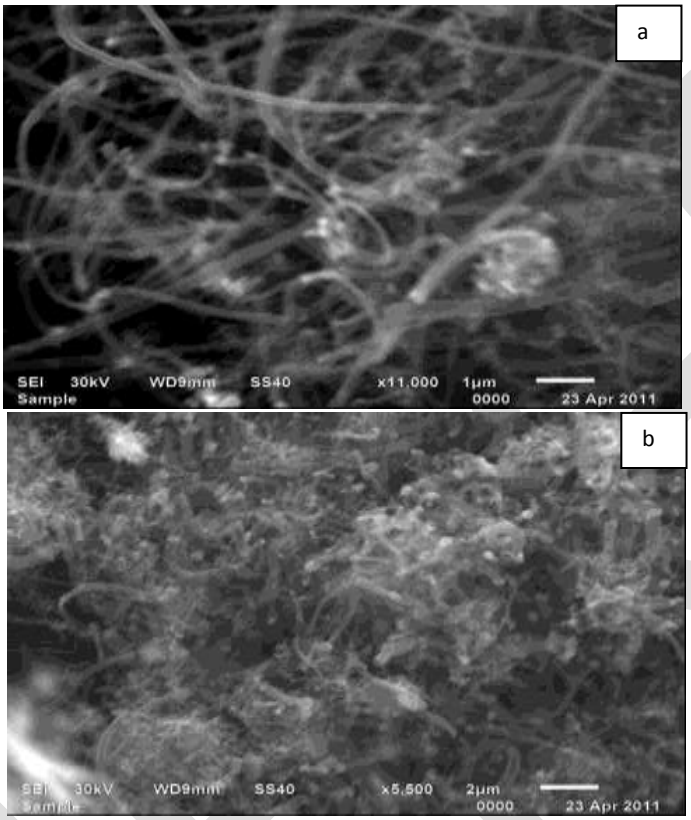

Fig .5. SEM image of CNTs produced over
(a) CuO –CeO_2- Fe_2O_3- Al_2O_3 (b) CuO –Fe_2O_3

TEM image of the produced CNTs over both CuO -Fe_2O_3 and CuO-Fe_2O_3 -CeO_2-Al_2O_3 are shown in Fig. 6. Graphitic structures with a central channel (CNTs) are observed and we observe also that the carbon nanotubes are thicker over CuO-Fe_2O_3 which has larger crystal size in agreement with SEM image.

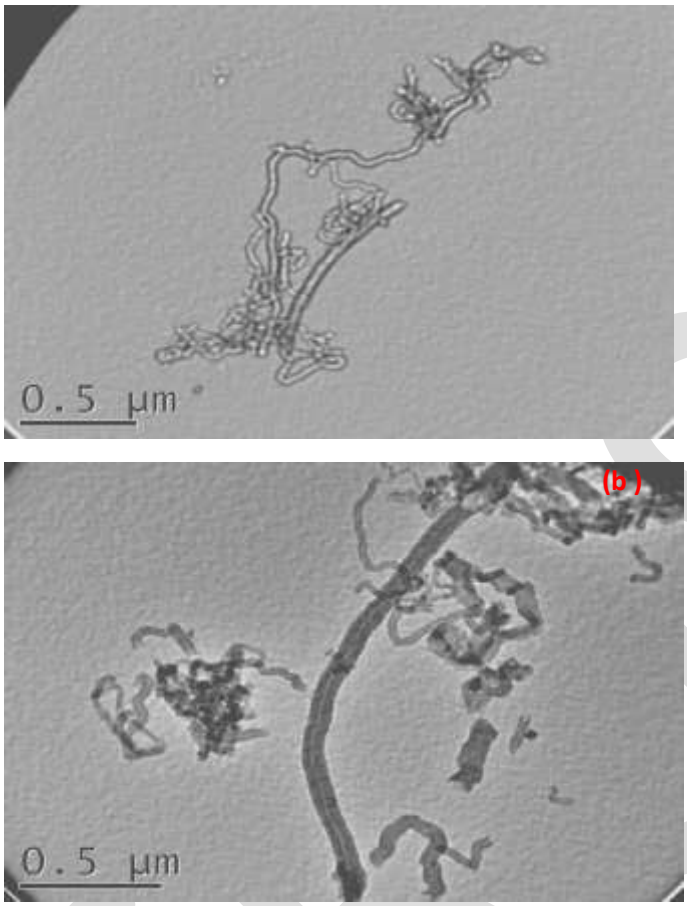

Fig. 6. TEM image of CNTs produced over
(a) CuO –CeO_2- Fe_2O_3- Al_2O_3 (b) CuO –Fe_2O_3

The produced CNTs are also investigated by XRD as shown in Fig. 7. for CuO -Fe_2O_3 and CuO-Fe_2O_3-CeO_2-Al_2O_3 samples after decomposition of acetylene. the XRD patterns cannot differentiate between CNTs and other similar graphite-like structures, since the diffraction peaks of both CNTs and graphite are very close to each other[29], but they provide a primary evidence of graphite formed. XRD patterns of the catalysts after acetylene decomposition shows that there are two major peaks, one is near $2\theta = 26^o$ And one near $2\theta = 43.5^o$ for graphite, indicating the well graphitized nature of the CNT. The other major peaks are due to catalytic impurities, Fe_3O_4 , CuO , Ce_2O_3, $CuFe_2O_4$ phases and Al_2O_3,the lower metal oxides is formed from the reduction of the metal oxides by acetylene and hydrogen formed from the decomposition of acetylene to hydrogen and CNTs.

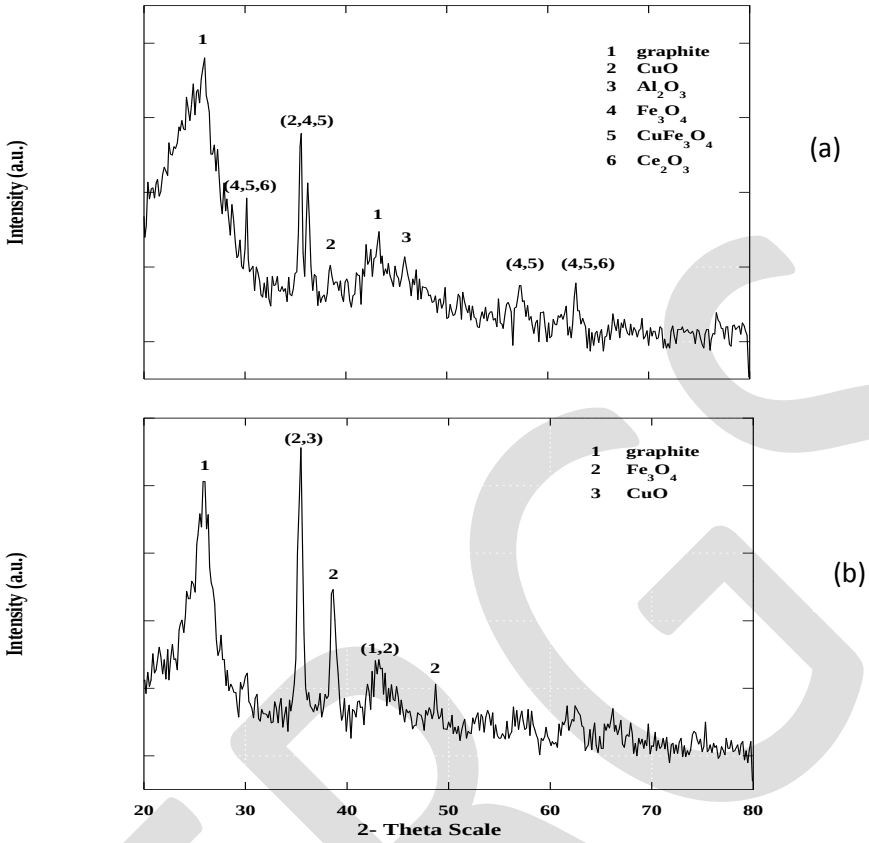

Fig.7. XRD patterns of CNTs after decomposition of acetylene at 600 ^{o}C over:
(a) CuO-Fe_2O_3 -CeO_2-Al_2O_3 (b) CuO-Fe_2O_3

3.2.2. Kinetic and mechanism of acetylene decomposition

To study the kinetics and mechanism of acetylene decomposition over CuO -Fe_2O_3 and CuO-Fe_2O_3-CeO_2-Al_2O_3, series of decomposition experiment were carried out in the temperature range of 400-600 ^{o}C. Fig. 8. Shows the effect of temperature on the conversion% of acetylene and it was found that the catalytic temperature is one of the most important factors that control the efficiency of catalytic reaction. Two modes of decomposition rate can be observed for CuO-Fe_2O_3 -CeO_2-Al_2O_3 catalyst fig. 8b. The first one at lower decomposition temperature, 400 and 450 ^{o}C, where the conversion percent 31% and 36.6 % was recorded, respectively. Increasing the temperature to 500 and 600 ^{o}C results a significant increase in the conversion percent and maximum percentage yield of 59.6 and 68 % were observed at 500 and 600 ^{o}C, respectively

As time proceeds, acetylene conversion% percent increase and the rate of conversion is high initially and slows down till the end of the reaction.

Fig.9. summarizes the effect of temperature on the acetylene conversion percent over Fe_2O_3-CuO and CuO-CeO_2-Fe_2O_3-Al_2O_3.

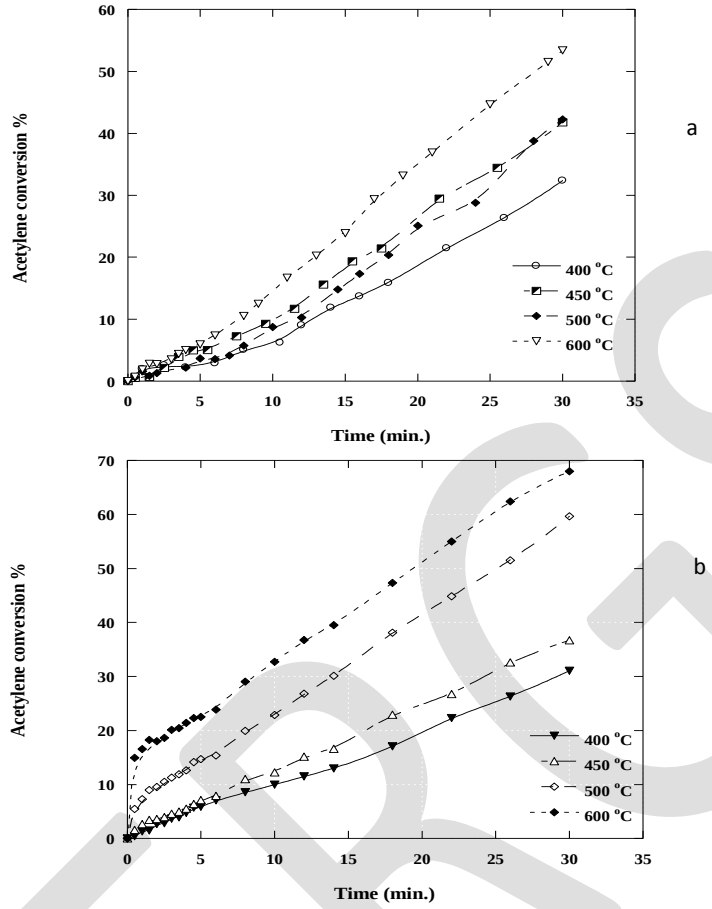

Fig.8. Effect of temperature on the catalytic decomposition of acetylene over
(a) $CuO\text{-}Fe_2O_3$ (b) $CuO\text{-}Fe_2O_3\text{-}CeO_2\text{-}Al_2O_3$

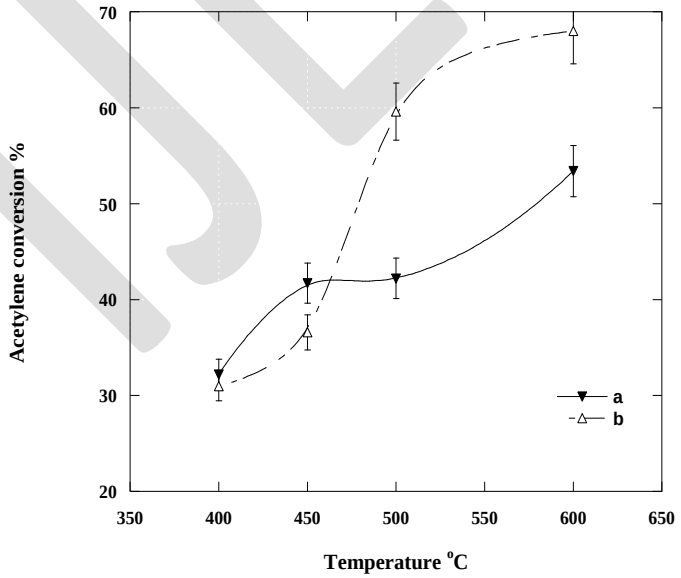

Fig.9. The relationship between the acetylene decomposition temperature and the HC conversion % over

(a) $CuO\text{-}Fe_2O_3$ (b) $CuO\text{-}Fe_2O_3\text{-}CeO_2\text{-}Al_2O_3$

Fig.10.represents the Arrhenius plot of CNTs synthesis, from which activation energy value was calculated. The small value of activation energy, 11.9 and 17.2 kJ/ mol ,for Fe_2O_3-CuO and $CuO\text{-}CeO_2\text{-}Fe_2O_3\text{-}Al_2O_3$ respectively, indicates that the two catalysts are very active toward acetylene decomposition.

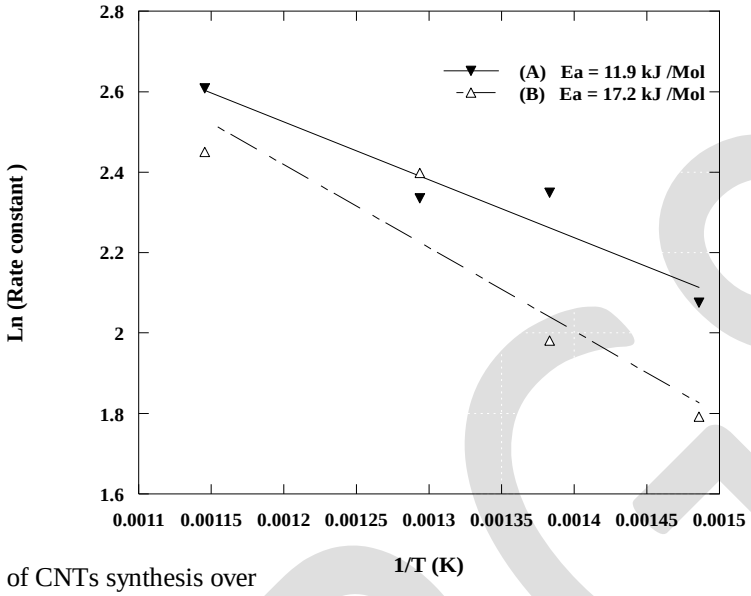

Fig.10: Arrhenius plot of CNTs synthesis over
(a) $CuO\text{-}Fe_2O_3$ (b) $CuO\text{-}Fe_2O_3\text{-}CeO_2\text{-}Al_2O_3$

3.2.3 Effect of acetylene flow rate

Effect of acetylene gas flow rate over 0.25 g of the most active catalyst on acetylene conversion % are given on table.4 and fig.11.It is apparent from the table that acetylene conversion % increase with the decrease of the acetylene flow rate and this may be attributed to that with increasing acetylene flow rate the CNTs yield is very high at the beginning of the reaction, covering and poisoning the active sites on the catalyst surface and consequently acetylene conversion percent decrease.

Table .4. Effect of gas flow rate on acetylene decomposition over $CuO\text{-}Fe_2O_3\text{-}CeO_2\text{-}Al_2O_3$

Gas Flow rate	150 ml/min	100 ml/min	50 ml/min
HC conversion %	30 %	50%	60%

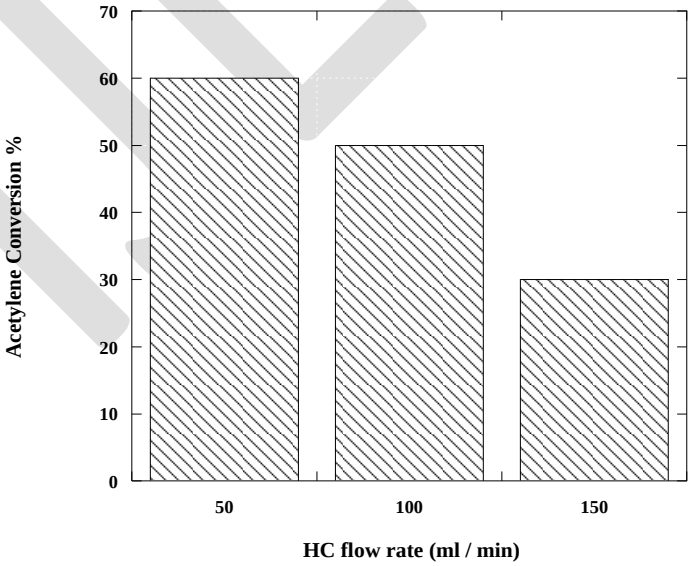

Fig.11. Histogram of the HC conversion % and acetylene flow rate over $CuO\text{-}Fe_2O_3\text{-}CeO_2\text{-}Al_2O_3$ catalysts at 600°C

3.2.4. Effect of catalyst weight

Effect of weight of $CuO\text{-}CeO_2\text{-}Fe_2O_3\text{-}Al_2O_3$ catalyst on acetylene conversion % using 50 ml/min gas flow rate are given in table .5 and fig.12.

Table .5. Effect of catalyst weight on acetylene decompositionover $CuO\text{-}Fe_2O_3\text{ -}CeO_2\text{-}Al_2O_3$

Catalyst weight	0.25 gram	0.5 gram	1 gram	2 gram
HC conversion %	60 %	68 %	77 %	42%

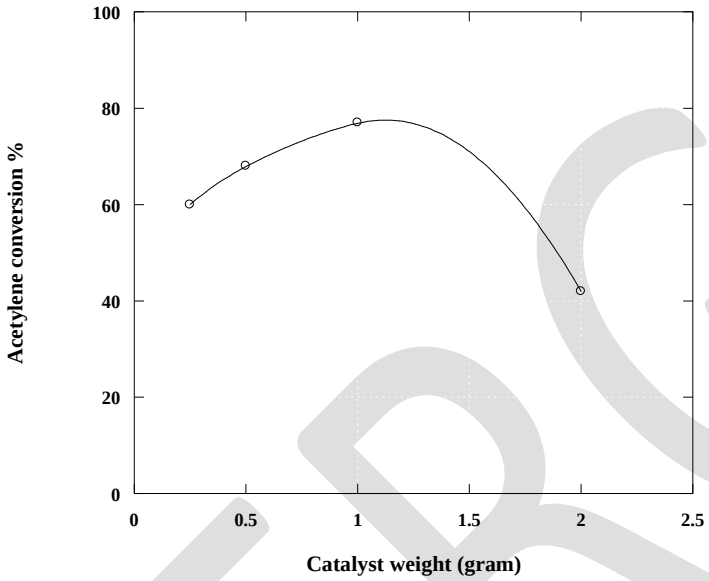

Fig.12. Effect of weight of $CuO\text{ –}CeO_2\text{- }Fe_2O_3\text{- }Al_2O_3$ on hydrocarbon conversion % using 50ml/min gas flow rate

It is apparent that the catalytic activity increase with increasing weight from 0.25 to 1 g because this metal loading exhibit the formation of CNTs having highest resistance to oxidation and also catalytically active sites are introduced in the system. with further increase on the catalyst's weight ,CNTs formed were more readily to oxidized and consequently the carbon deposited will decrease and the conversion percent decrease [7].

Conclusion

Nanosized $CuO\text{-}CeO_2$, $CuO\text{-}Fe_2O_3$, $CuO\text{-}CeO_2\text{-}Al_2O_3$ and $CuO\text{-}Fe_2O_3\text{-}CeO_2\text{-}Al_2O_3$ were prepared by co-precipitation and wet impregnations techniques and were used for Catalytic decomposition of acetylene to produce carbon nanotubes (CNTs). Weight gain technique was used to follow up the catalytic reactions. The results revealed that catalyst chemical composition, catalytic temperature, acetylene flow rate and catalyst's weight have a significant effect on the acetylene conversion percent. It was found that maximum acetylene conversion% occurs over $CuO\text{-}CeO_2\text{-}Fe_2O_3\text{-}Al_2O_3$ and $CuO\text{-}Fe_2O_3$ and it increase by increasing, temperature from 400-600^oC, decreasing acetylene flow rate from 150-50 ml/min and increasing catalyst weight from 0.25-1g. With further increase in catalyst weight, acetylene conversion% decrease. The SEM image shows that some catalytic nanoparticales are observed at the tips of the carbon nanotubes indicating that CNTs formation occurs via tip growth mechanism. The results show that nanocrystallite $CuO\text{-}Fe_2O_3\text{ -}CeO_2\text{-}Al_2O_3$ can be recommended as promising catalysts for hydrocarbon decomposition.

REFERENCES:

[1] A. GLOBAL .Quantification of the disease burden attributable to environmental risk factors.

[2] C. Mathers, G. Stevens, M. Mascarenhas, Global health risks: mortality and burden of disease attributable to selected major risks, World Health Organization, 2009.
[3] H. Rodhe, Science 248 (1990) 1217-1219.
[4] B.J. Finlayson-Pitts, J.N. Pitts, Science 276 (1997) 1045-1051.
[5] M.F. Zwinkels, S.G. Järås, P.G. Menon, T.A. Griffin, Catalysis Reviews Science and Engineering 35 (1993) 319-358.
[6] M. Khedr, K. Abdel Halim, N. Soliman, Applied Surface Science 255 (2008) 2375-2381.
[7] T. Tsoufis, P. Xidas, L. Jankovic, D. Gournis, A. Saranti, T. Bakas, M.A. Karakassides, Diamond and related materials 16 (2007) 155-160.
[8] S. Iijima, nature 354 (1991) 56-58.
[9] J. Robertson, Materials Today 7 (2004) 46-52.
[10] Y. Zhang, Y. Bai, B. Yan, Drug Discovery Today 15 428-435.
[11] K. Gong, Y. Yan, M. Zhang, L. Su, S. Xiong, L. Mao, Analytical sciences: the international journal of the Japan Society for Analytical Chemistry 21 (2005) 1383-1393.
[12] A. Hassanien, M. Tokumoto, Y. Kumazawa, H. Kataura, Y. Maniwa, S. Suzuki, Y. Achiba, Applied physics letters 73 (1998) 3839-3841.
[13] A.Y. Kasumov, R. Deblock, M. Kociak, B. Reulet, H. Bouchiat, I. Khodos, Y.B. Gorbatov, V. Volkov, C. Journet, M. Burghard, Science 284 (1999) 1508-1511.
[14] R. Rakhi, K. Sethupathi, S. Ramaprabhu, Carbon 46 (2008) 1656-1663.
[15] H.D. Lim, K.Y. Park, H. Song, E.Y. Jang, H. Gwon, J. Kim, Y.H. Kim, M.r.D. Lima, R.O. Robles, X. LeprÃ³, Advanced Materials 25 1348-1352.
[16] Y.-S. Kim, K. Kumar, F.T. Fisher, E.-H. Yang, Nanotechnology 23 015301.
[17] W.-P. Dow, Y.-P. Wang, T.-J. Huang, Applied Catalysis A: General 190 (2000) 25-34.
[18] Y. Ando, X. Zhao, T. Sugai, M. Kumar, Materials Today 7 (2004) 22-29.
[19] M. Perez-Cabero, E. Romeo, C. Royo, A. Monzón, A. Guerrero-Ruiz, I. Rodríguez-Ramos, Journal of catalysis 224 (2004) 197-205.
[20] T. Ebbesen, H. Lezec, H. Hiura, J. Bennett, H. Ghaemi, T. Thio, (1996).
[21] H. Dai, J.H. Hafner, A.G. Rinzler, D.T. Colbert, R.E. Smalley, Nature 384 (1996) 147-150.
[22] J. Cheng, X. Zhang, Z. Luo, F. Liu, Y. Ye, W. Yin, W. Liu, Y. Han, Materials chemistry and physics 95 (2006) 5-11.
[23] B.D. Cullity, S.R. Stock, Elements of X-ray Diffraction, Prentice hall Upper Saddle River, NJ, 2001.
[24] C.R. Jung, J. Han, S. Nam, T.-H. Lim, S.-A. Hong, H.-I. Lee, Catalysis today 93 (2004) 183-190.
[25] G. Avgouropoulos, T. Ioannides, H. Matralis, Applied Catalysis B: Environmental 56 (2005) 87-93.
[26] S. Li, C. Wu, H. Li, B. Li, Reaction Kinetics and Catalysis Letters 69 (2000) 105-113.
[27] A. Fazle Kibria, Y. Mo, K. Nahm, M. Kim, Carbon 40 (2002) 1241-1247.
[28] K. Kuwana, H. Endo, K. Saito, D. Qian, R. Andrews, E.A. Grulke, Carbon 43 (2005) 253-260.
[29] W. Zhu, D. Miser, W. Chan, M. Hajaligol, Materials chemistry and physics 82 (2003) 638-647